Plasmonics (2024) 19:439–445
https://doi.org/10.1007/s11468-023-02014-5

RESEARCH

Photonic Crystal based Biosensor for Diagnosis of Kidney Failure and Diabetes

Esmat Rafiee[1]

Received: 7 August 2023 / Accepted: 18 August 2023 / Published online: 23 August 2023

Abstract

In this work, a biosensor based on two-dimensional photonic crystals is proposed. The structure is based on 30*20 silicon rods on the air background. The structure is considered for detection of Glucose and Creatinine concentrations in blood samples. This can help physicians in diagnosis of diabetes and kidney failure. The proposed biosensor is designed based on only linear materials to overcome low gain and nonlinearity difficulties. The functionality of the biosensor is fulfilled by considering the interference and scattering effects of Si defect rod situated in the structure (dark blue rods function as confining sensing media while dark green rods act as coupling rods). The proposed biosensor is designed in the format of hexagon shaped rings; filtering the operating resonance wavelengths. The functionality of the presented biosensor is investigated by considering the photonic band gap (PBG) and field distribution spectra, through the plane wave expansion (PWE) and finite-difference-time-domain (FDTD) methods. The incident light wave would be applied to the input port and according to the resonant wavelength would be transmitted to Outputs 1 or 2. The dimension of the proposed structure is considered as $114\mu m^2$ which makes it an appropriate option for optical integrated circuits. Finally, for Glucose, the remarkable sensitivity (*1400 nm/RIU*), quality factor (*163.6—169.8*), detection limit (*6.6e-4—6.8e-4*) *RIU* and figure of merit (*150.4—152.*6) RIU^{-1} were obtained. Similarly, for Creatinine, the sensitivity (*795 nm/RIU*), quality factor (*53.5—58*), detection limit (*0.0029—0.0030*) *RIU* and figure of merit (*33.07—34.56*) RIU^{-1} were achieved.

Keywords Biosensor · Creatinine · Glucose · Optical integrated circuit · Photonic crystal · Refractive index

Introduction

Recently, optical structures have been the main field of research interest for various scientists. This happens due to their compact sizes, very low costs (compared with conventional technologies), extremely higher capacities and speeds (compared with electronic based devices). This is mainly due to the fact that in optical based devices, electrons (which are responsible for electronic device's operations) are replaced by photons (which are responsible for optical device's operations) [1–3]. Very high speed of light with other advantages attracted the attentions of many researchers (to the optical based devices). As a result, all of the elements considered in electronic circuits should be converted to optical ones (elements like, logic gates, filters, sensors or biosensors, receivers, transmitters and etc.) [4–7]. Photonic crystals (PhCs) are optical based devices which are periodic in one, two or three dimensions. They are basically made of at least two individual media (i.e. air and a dielectric) in a periodic (circular, hexagonal, cubic, etc.) pattern. PhCs in most configurations are defined by periodic cells (rods) in the background made of air. All of the materials utilized in PhC based devices and generally in optical structures are defined by their refractive indices (RIs). In fact, refractive index is the main identification factor for materials used in the designation of optical integrated circuits (OICs). The periodicity of the PhC based structures can be defined by the lattice constant parameter, which indicates the distance between adjacent rods [8]. An important parameter defining the functionality of the PhC based structure is the photonic bandgap (PBG). In fact, PBG diagram is a spectrum which shows regions of frequency (wavelength), where light can be transmitted or not. As a matter of fact, these regions are denoted as the forbidden (non-guided) or permitted (guided) regions. For different PhC based structures, by

✉ Esmat Rafiee
e.rafiee@alzahra.ac.ir

[1] Department of Electrical Engineering, Faculty of Engineering, Alzahra University, Tehran, Iran

considering plane wave expansion (PWE) method, PBG can be obtained. In different applications, wavelengths (frequencies) situated in the forbidden or permitted regions can be considered. Mostly, signals with permitted wavelengths would be propagated in the PhC structure and would be eventually dispersed. Finally, they would lose their energies. On the other hand, signals with forbidden wavelengths wouldn't be propagated in the PhC structure. They would be reflected in the structure after hitting other opposite side rods (this happens along the waveguide). Therefore, in the latter case total internal reflection (TIR) effect can help the light wave propagate along the waveguide with very low losses [9–13]. PhC based structures can be designed for various OICs. Elements like logic gates, filters, splitters, receivers, biosensors, transmitters and etc. can be designed by PhCs. PhC-based structures can be specially considered in designation of various sensors. Gas and liquid sensors are among the most important categories of PhC- based sensors [14]. Optical biosensors have attracted attentions of many researchers due to their compact size, integrability, ease of fabrication and high speed and can be designed based on various configurations [15].

Bio-optoelectronic structures can also take advantage of the benefits of optical structures [16, 17]. PhC based devices can be configured as biosensors for detection of various biological elements in blood samples [18, 19]. For diagnosing diabetes, Glucose concentration in blood samples should be considered (high levels of Glucose increase the risk of diabetes). In order to diagnose kidney failure, creatinine concentration should be measured (high levels of Creatinine may cause kidney failure) [20–22]. As stated, many researchers have reported their works on optical biosensors. In a research [23], a PhC- based biosensor with the sensitivity and limit of detection of 260 nm/RIU and 0.001 RIU, respectively, was proposed. In [24], ring resonators based on PhC structures were reported for detection of cancer cells. In another research [25], by considering layers of metal/defect/metal in the photonic crystal configuration, a biosensor for diagnosis of malaria was proposed. In [26], by considering irregular defects in the PhC structure, a biosensor for detection of blood plasma was suggested. Recently [27], a PhC based biosensor was considered and analyzed for diagnosing biomolecules in urine and blood. In another work [28], 2-D PhC based biosensor was considered for diagnosis of DNA. In [29], by using $Ti_3C_2T_x$ MXene material in a D-shaped PhC fiber, a sensitive biosensor was designed. In [30], by detecting plasma, platelets, red blood cell and uric acid in blood samples, chikunguniya virus was detected. The proposed biosensor was based on 2-D PhC structures [30]. In another research [31], a biosensor based on photonic crystal fiber in the shape of rectangular core was proposed which could diagnose red blood cell (RBC), white blood cell (WBC), plasma, water and Hemoglobin. This research proposes a simple, easy fabricated, integrable and functional biosensor by considering 2D PhCs. The proposed structure is utilized for detection of Glucose and Creatinine concentrations in blood samples (diagnosing diabetes and kidney failure). The PBG diagram and field distribution at the two individual output ports are considered. Eventually, the structure is considered as biosensors for detection of Glucose and Creatinine at outputs 1 and 2, respectively. In the following parts, first the methodology and design section (the proposed biosensor and its functionality), then the simulations and results (considering filed distribution and transmission-wavelength spectrum for various Glucose and Creatinine concentrations at outputs 1 and 2) and finally the conclusion section are presented.

Methodology and Design

In this work, a 30*20 biosensor based on PhCs is being designed and investigated. For investigating the functionalities of the proposed structure, PBG diagram and field distributions should be studied which can be conducted by considering Maxwell's equations.

$$\frac{\partial B}{\partial t} = -\nabla * E - J \tag{1}$$

$$\frac{\partial B}{\partial t} = \nabla * H - J \tag{2}$$

where E, H, D, B and J indicate the electric field, magnetic field, electric displacement, magnetic induction fields and electric-charge current density, respectively.

Plane wave expansion (PWE) and finite difference time domain (FDTD) methods can be considered for extracting the PBG and field distribution diagrams, respectively [32, 33]. There are some important parameters which should be calculated and analyzed for defining the functionality of a biosensor. Quality factor (Q) is one of these parameters which is presented in the following equation [7, 34].

$$Q = \frac{\lambda_0}{\Delta\lambda_{FWHM}} \tag{3}$$

in which λ_0 and $\Delta\lambda_{FWHM}$, stand for the resonant wavelength and spectral with of half maximum for the central transmission spectrum, respectively. Sensitivity (S) is another important parameter defining the least possible detectable changes in the refractive index of the sensing medium.

$$S = \frac{\Delta\lambda}{\Delta n}(nm/RIU) \tag{4}$$

where $\Delta\lambda$ and Δn define the transmission spectrum displacement and changes of the RI, respectively. Its unit is mostly stated as "*nm/RIU*". Detection limit (DL) is another important parameter which is defined as below:

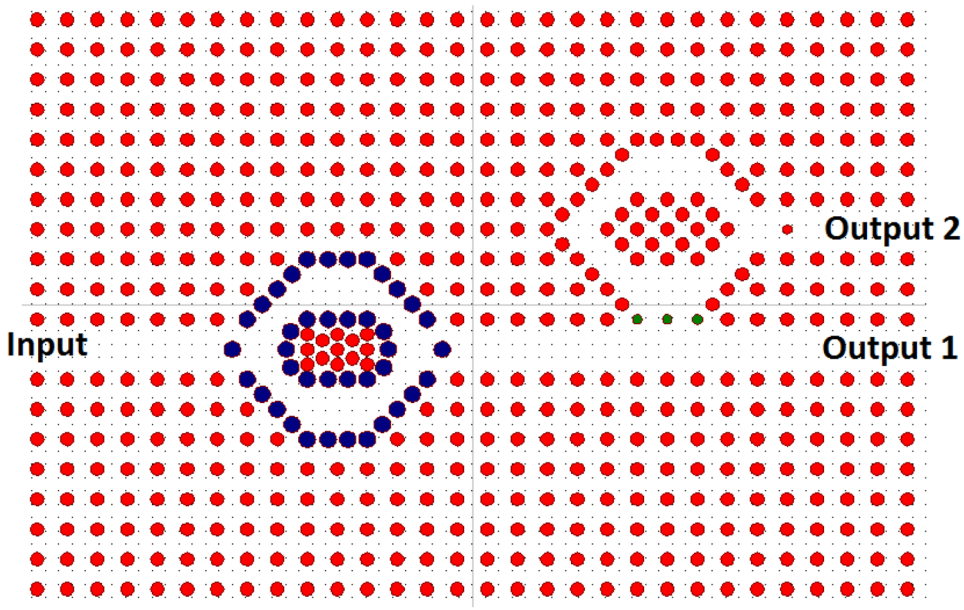

Fig. 1 The proposed biosensor based on 2-D PhCs

$$DL = \frac{\lambda}{10SQ}(RIU) \tag{5}$$

In which λ, S and Q stand for the resonant wavelength, sensitivity and quality factor, respectively.

Figure of merit (*FOM*) is also another important parameter presented in Eq. (6).

$$FOM = \frac{SQ}{\lambda}(RIU^{-1}) \tag{6}$$

where S, Q and λ stand for sensitivity, quality factor and resonant wavelength, respectively [7, 34].

The proposed 2-D PhC based biosensor can be seen in Fig. 1.

As can be seen in Fig. 1, the proposed structure is consisted of 30*20 Si rods in the background of air. In order to make the structure functional and simple (designation and fabrication), only linear rods were considered. Line defects (omitting rods to form the Input, Output1 and Output2 pathways) and point defects (dark blue and dark green rods) were considered in the structure for ease of functionality. Dark blue rods act as the confining sensing media (reflecting rods) and are in contact with the tested materials (the hexagon shaped ring help filter the operating resonance frequency). Dark green rods function as the coupling rods filter the appropriate wavelengths for the Output2 port. The structural parameters of Fig. 1 are tabulated in Table. 1.

Table 1 Structural parameters of Fig. 1

Parameter	Value
Red rod's radius	*0.1 μm*
Dark blue rod's radius	*0.125 μm*
Dark green rod's radius	*0.8 μm*
Lattice constant (a)	*0.45 μm*
Refractive index of rods	*3.5*

In the first step of a 2-D PhC based biosensor designation, the PBG diagram should be presented. PBG spectrum of the proposed biosensor can be seen in Fig. 2.

As seen in Fig. 2, TE and TM modes were extracted for the proposed biosensor. TE modes are obtained in the wavelength ranges of $1.14\ \mu m < \lambda < 1.895\ \mu m$ and $0.813\ \mu m < \lambda < 0.93\ \mu m$. TM modes are also achieved in the wavelength range of $0.75\ \mu m < \lambda < 0.935\ \mu m$.

TE mode is considered for further simulations due to its wider and more dominant wavelength range. In the TE mode range, the light wave can be propagated through

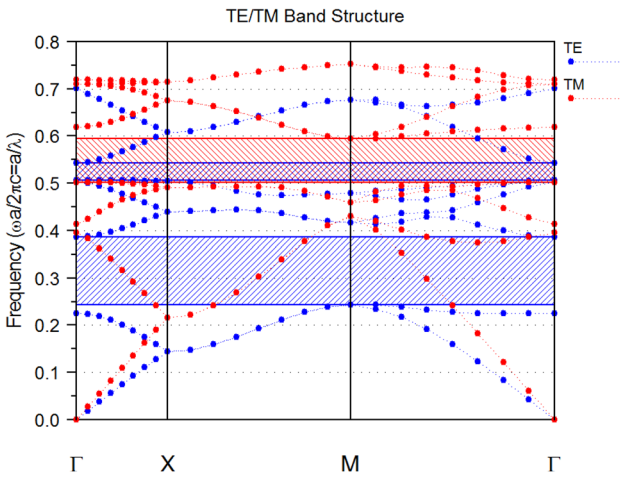

Fig. 2 View of the PBG of the proposed biosensor

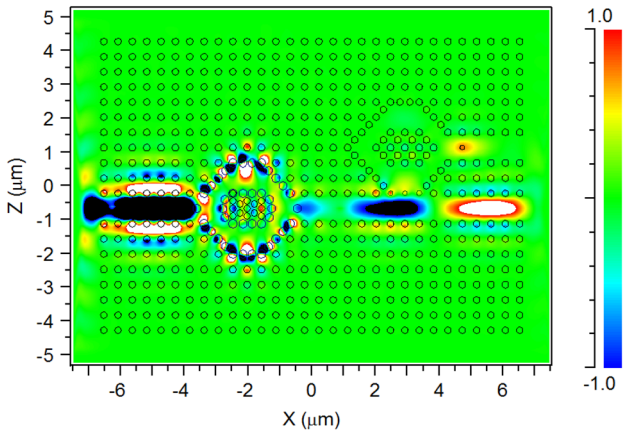

Fig. 3 Field distribution at $\lambda = 1550\ nm$

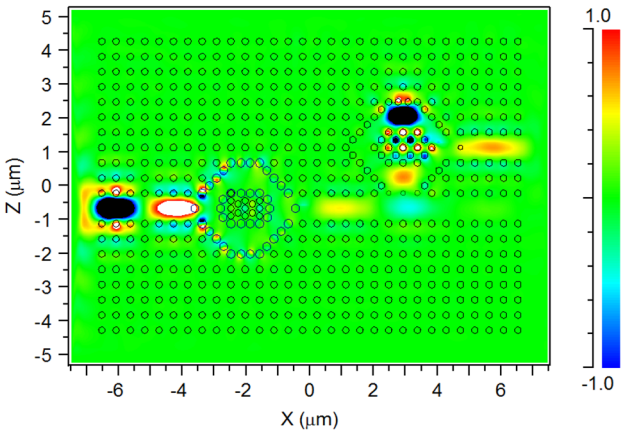

Fig. 5 Field distribution at $\lambda = 1290\ nm$

the structure (without being dispersed) by considering the total internal reflection effect (TIR). As a result, for the following simulations, the wavelengths situated in the PBG range would be considered as the input wavelength (for having the TIR effect). In order to have biosensors with the ability of detecting Creatinine and Glucose at individual output ports, various simulations with different input central wavelengths should be conducted.

In the following parts, first, field distributions at $\lambda = 1550\ nm$ and $\lambda = 1290\ nm$ for Outputs 1 and 2 are obtained. Then, by considering different concentrations of Creatinine and Glucose, their effects on the resonant wavelength are considered (transmission-wavelength for different RIs were depicted). Finally, *Q*, *S*, *DL* and *FOM* parameters are calculated.

Simulations and Results

In this part by considering the incident field at different wavelengths (in the TE range), field distributions and transmission-wavelength spectra are obtained.

Output 1 ($\lambda = 1550\ nm$)

In this section, by considering $\lambda = 1550\ nm$, the light wave would be transmitted to Output1 as shown in Fig. 3.

As seen, most of the incident light wave would be transmitted to Output1 at $\lambda = 1550\ nm$. In this section, by considering different concentrations of Glucose in blood samples (by their RIs), transmission spectrum versus wavelength would be obtained. Diabetes can be diagnosed by

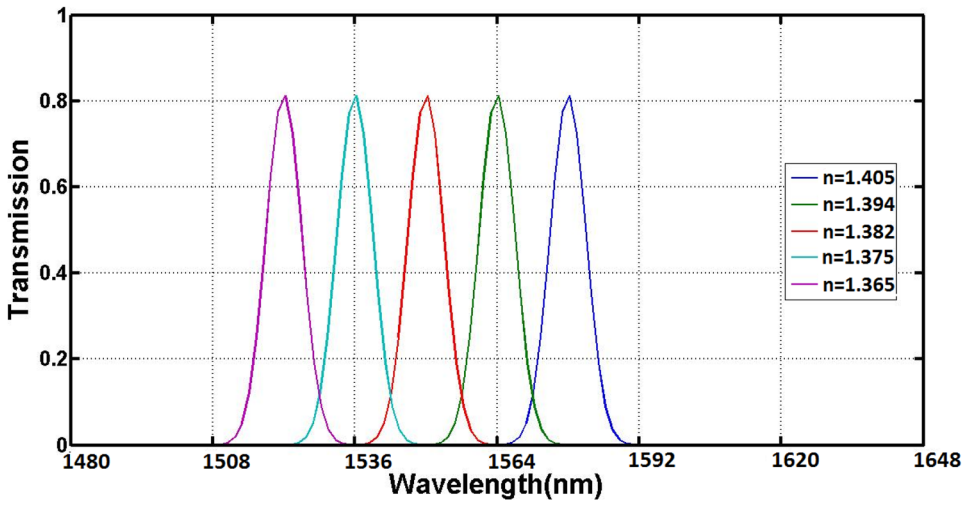

Fig. 4 Transmission spectrum vs. wavelength for various Glucose concentrations

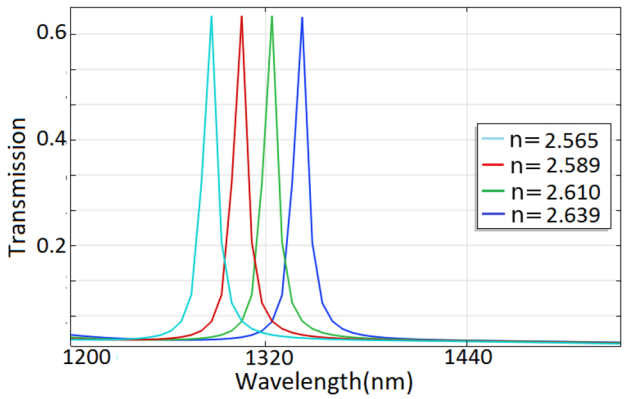

Fig. 6 Transmission spectrum vs. wavelength for various Creatinine concentrations

considering the obtained results (for people with different genders, ages and etc., specific values of Glucose concentrations can lead to diabetes). The following figure indicates the evolutions of the resonant wavelength by considering various concentrations of Glucose (defined by RIs) in blood samples.

Considering Fig. 4, the utilized RIs of *1.365*, *1.375*, *1.382*, *1.394* and *1.405* are related to various Glucose concentrations in blood samples ($n = 1.365$ for *75 mg/dl*, $n = 1.375$ for *100 mg/dl*, $n = 1.382$ for *125 mg/dl*, $n = 1.394$ for *150md/dl* and $n = 1.405$ for *175 mg/dl* [35]). As seen in Fig. 4, increasing RI would lead the transmission's peak wavelength to higher values (red-shift) [18, 36].

By considering Fig. 4 and Eqs. (3–6), the following parameters for the biosensor at Output1 can be obtained. Quality factor (*Q*): (*163.6—169.8*), Sensitivity (*S*): *1400 nm/RIU*, detection limit (*DL*): (*6.6e-4—6.8e-4*) *RIU*, Figure of merit (*FOM*): (*150.4–152.6*) RIU^{-1}.

Finally, by considering wavelengths in the range of $1522\ nm < \lambda < 1578\ nm$, the mentioned concentrations of Glucose in blood samples can be detected. This can help in diagnosis of diabetes. In the following part, by considering incident field with $\lambda = 1290\ nm$, various concentrations of Creatinine in blood samples at Output2 would be diagnosed.

Output 2 ($\lambda = 1290\ nm$)

In this section, by considering $\lambda = 1290\ nm$, the light wave would be transmitted to Output2 as shown in Fig. 5.

As shown in Fig. 5, most of the incident light wave was transferred to Output2 at $\lambda = 1290\ nm$. In this part, by considering various concentrations of Creatinine in blood samples (by their RIs), transmission spectrum versus wavelength could be obtained. Kidney failure diseases can be diagnosed by considering the obtained results (for people with different genders, ages and etc., specific values of Creatinine concentrations can lead to kidney failure). The following diagram indicates the evolutions of the resonant wavelength by considering various concentrations of Creatinine (defined by RIs) in blood samples.

The utilized RIs of Fig. 6, are related to various Creatinine concentrations in blood samples ($n = 2.565$ for *85.28 µmol/L*, $n = 2.589$ for *84.07 µmol/L*, $n = 2.610$ for *83.3 µmol/L* and $n = 2.639$ for *82.3 µmol/L* [21]). It is obvious from Fig. 6, that increasing RI would move the transmission's peak wavelength to higher amounts [18, 36]. By considering Fig. 6 and Eqs. (3–6), the following parameters for the biosensor at Output2 can be obtained. Quality factor (*Q*): (*53.5—58*), Sensitivity (*S*): *795 nm/RIU*, detection limit (*DL*): (*0.0029—0.0030*) *RIU*, Figure of merit (*FOM*): (*33.07—34.56*) RIU^{-1}. Therefore, by considering wavelengths in the range of $1286\ nm < \lambda < 1344\ nm$, the mentioned concentrations of Creatinine in blood samples can be detected. This can help in diagnosis of kidney failure diseases. Results of the propped sensor were compared with previous published works and are tabulated in Table 2.

Table 2 Comparison of our suggested biosensor with published works

References	Sensitivity (*nm/RIU*)	FOM (RIU^{-1})	DL (*RIU*)	Q-Factor
Creatinine sensor [21]	*306*			
Creatinine sensor [37]	*42*			
Creatinine sensor [38]	*637*	*10.3*	*0.001*	
Creatinine sensor [39]	*75*	*26*		
Proposed Creatinine sensor	*795*	*33.07—34.56*	*0.0029—0.0030*	*53.5–58*
Glucose sensor [3]	*1278*	*105*		
Glucose sensor [40]	*225*	*20.45*		
Proposed Glucose sensor	*1400*	*150.4—152.6*	*6.6e-4—6.8e-4*	*163.6—169.8*

Conclusion

An efficient and compact biosensor based on 2-D PhCs was presented. The structure was designed based on 30*20 Si rods in the air background. For ease of fabrication and designation, only linear materials were considered. Various defect rods (dark blue and dark green rods) were responsible for the interference and scattering phenomena. They also confined light wave in the sensing medium. Application of the proposed structure was studied through PWE (extracting the PBG spectrum) and FDTD (extracting filed distribution diagram) methods. Output1 (operating at $\lambda = 1550\ nm$) was considered for detection of Glucose concentrations in blood samples. The remarkable *S*, *Q*, *FOM* and *DL* of *1400 nm/RIU*, (*163.6–169.8*), (*150.4–152.6*) RIU^{-1} and (*6.6e-4–6.8e-4*) *RIU* were achieved for Glucose concentration biosensor, respectively. In Output2 (operating at $\lambda = 1290\ nm$), Creatinine concentrations were detected with *S*, *Q*, *FOM* and *DL* of *795 nm/RIU*, (*53.5–58*), (*33.07–34.56*) RIU^{-1} and (*0.0029–0.0030*) *RIU*, respectively. Finally, by obtaining Glucose and Creatinine concentrations in blood samples, diabetes and kidney failure diseases can be diagnosed. The proposed biosensor can be a remarkable candidate for utilization in bio-optical integrated circuits.

Authors' Contributions Esmat Rafiee contributed to the study conception and design. Material preparation, data collection and analysis were performed by Esmat Rafiee. The manuscript was written by Esmat Rafiee.

Funding The authors declare that no funds, grants, or other support were received during the preparation of this manuscript.

Data Availability Not applicable.

Declarations

Ethical Approval Not applicable.

Conflict of Interests The authors declare that they have no conflict of interest. The authors have no relevant financial or non-financial interests to disclose.

References

1. Parandin F, Sheykhian A (2022) Design and simulation of a 2 × 1 All-Optical multiplexer based on photonic crystals. Opt Laser Technol 151:108021
2. Rafiee E, Emami F (2017) Design of a Novel All-Optical Ring Shaped Demultiplexer based on Two-Dimensional Photonic Crystals. Optik 140:873–877
3. Parandin F (2019) High contrast ratio all-optical 4 × 2 encoder based on two-dimensional photonic crystals. Opt Laser Technol 113:447–452
4. Rafiee E, Emami F (2018) Realization of tunable optical channel drop filter based on photonic crystal octagonal shaped structure. Optik 171:798–802
5. Rafiee E et al (2018) Design of a Novel Nano Plasmonic-Dielectric Photonic Crystal Power Splitter Suitable for Photonic Integrated Circuits. Optik 172:234–240
6. Parandin F, Kamarian R, Jomour M (2021) A novel design of all optical half-subtractor using a square lattice photonic crystals. Opt Quant Electron 53:114
7. Parandin F et al (2022) Design of 2D photonic crystal biosensor to detect blood Components. Opt Quant Electron 54:618
8. Palai G et al (2017) Optical MUX/DEMUX using 3D photonic crystal structure: A future application of silicon photonics. Optik 128:224–227
9. Vahdati A, Parandin F (2019) Antenna patch design using a photonic crystal substrate at a frequency of 1.6 THz. Wireless Pers. Commun 109:2213–2219
10. Parandin F, Moayed M (2020) Designing and simulation of 3-input majority gate based on two-dimensional photonic crystals. Optik 216:164930. https://doi.org/10.1016/j.ijleo.2020.164930
11. Parandin F (2021) Ultra-compact terahertz all-optical logic comparator on GaAs photonic crystal platform. Opt Laser Technol 144:107399. https://doi.org/10.1016/j.optlastec.2021.107399
12. Parandin F, Heidari F, Rahimi Z, Olyaee S (2021) Two-dimensional photonic crystal Biosensors: A review Opt Laser Technol 144:107397. https://doi.org/10.1016/j.optlastec.2021.107397
13. Askarian A (2021) Design and analysis of all optical 2 × 4 decoder based on kerr effect and beams interference procedure. Opt Quant Electron 53:291
14. Zhao Y et al (2011) Research advances of photonic crystal gas and liquid sensors. Sens Actuators B 160:1288–1297
15. Scullion MG et al (2013) Slotted Photonic Crystal Sensors Sensors. 13:3675–3710. https://doi.org/10.3390/s130303675
16. Rafiee E et al (2023) Cancer Cell Detection Biosensor Based on Graphene-Plasmonic Split Square-Ring-Shaped Nanostructure. Plasmonics 18:431–440
17. Negahdari R et al (2023) A Sensitive Biosensor Based on Plasmonic-Graphene Configuration for Detection of COVID-19 Virus. Plasmonics
18. Chahkoutahi A et al (2022) Sensitive Hemoglobin Concentration Sensor Based on Graphene-Plasmonic Nano-structures. Plasmonics 17:423–431
19. Negahdari R et al (2023) Sensitive MIM plasmonic biosensors for detection of hemoglobin, creatinine and cholesterol concentrations. Diam Relat Mater 136:110029
20. Panda A (2020) Performance analysis of graphene-based surface plasmon resonance biosensor for blood glucose and gas detection. Appl Phys A 126. https://doi.org/10.1007/s00339-020-3328-8.
21. Aly AH, Mohamed D, Mohaseb MA, Abd El-Gawaad NS, Trabelsi Y (2020) Biophotonic sensor for the detection of creatinine concentration in blood serum based on 1D photonic crystal. RSC Adv 10:31765. https://doi.org/10.1039/D0RA05448H.
22. Jin YL, Chen JY, Xu L, Wang PN (2006) Refractive index measurement for biomaterial samples by total internal reflection. Phys Med Biol 51:371–379. https://doi.org/10.1088/0031-9155/51/20/N02
23. Dutta HS et al (2013) Design of a highly sensitive photonic crystal waveguide platform for refractive index based biosensing. Opt Quantum Electron 45:907–917
24. Baraty F et al (2023) Label-Free cancer cell biosensor based on photonic crystal ring resonator. Results in Physics 46:106317
25. Ankita et al., An Improved Optical Biosensor design using defect/metal multilayer photonic crystal for Malaria Diagnosis. Results in Optics. 9:100304.

26. Kaviani H et al (2022) Photonic crystal based biosensor with the irregular defect for detection of blood plasma. Appl Surf Sci 599:153743
27. Yashaswini PR et al (2023) Performance analysis of photonic crystal based biosensor for the detection of bio-molecules in urine and blood. Materials Today: Proceedings 80(3):2247–2254
28. Benmerkhi A et al (2020) Design of two-dimensional photonic crystal biosensor using DNA detection. Phosphorus Sulfur Silicon Relat Elem 195(11):960–964
29. Kumar A et al (2022) Surface plasmon resonance biosensor based on a D-shaped photonic crystal fiber using Ti3C2Tx MXene material. Opt Mater 128:112397
30. Sharma S et al (2021) 2D photonic crystal based biosensor for the detection of chikungunya virus. Optik 237:166575
31. Al-Mamun Bulbul A et al (2021) Photonic crystal fiber-based blood components detection in THz regime: Design and simulation. Sensors International 2:100081
32. Gao YF et al (2010) Design of novel power splitters by directional coupling between photonic crystal waveguides. Optoelectron Lett 6:417–420. https://doi.org/10.1007/s11801-010-0017-4
33. Elyasi B, Javahernia S (2022) All optical digital multiplexer using nonlinear photonic crystal ring resonators. JOPN 7(1):97–106
34. Olyaeea S. Mohebzadeh-Bahabady et al (2014) Two-curve-shaped biosensor using photonic crystal nano-ring resonators. JNS 4:303–308
35. Panda A, Pukhrambam PD, Keiser G (2020) Performance analysis of graphene-based surface plasmon resonance biosensor for blood glucose and gas detection. Appl Phys A 126. https://doi.org/10.1007/s00339-020-3328-8.
36. Chorsi HT et al (2017) Tunable plasmonic substrates with ultrahigh Q-factor resonances. Sci Rep 7:15985
37. Ramanujam NR, Amiri IS, Taya SA, Olyaee S, Udaiyakumar R, Pandian AP, Joseph Wilson KS, Mahalakshmi P, Yupapin PP (2019) Enhanced sensitivity of cancer cell using one dimensional nano composite material coated photonic crystal. Microsyst Technol 25:189–196.
38. Gandhi S, Awasthi SK, Aly AH (2021) Biophotonic sensor design using a 1D defective annular photonic crystal for the detection of creatinine concentration in blood serum. RSC Adv 11:26655–26665
39. Bijalwan A, Singh BK, Rastogi V (2021) Analysis of one-dimensional photonic crystal based sensor for detection of blood plasma and cancer cells. Optik 226:165994
40. Vafapour Z (2019) Polarization-Independent Perfect Optical Metamaterial Absorber as a Glucose Sensor in Food Industry Applications. IEEE Trans Nanobioscience 18:622–627. https://doi.org/10.1109/TNB.2019.2929802